STRESS INTENSITY FACTOR FOR DOUBLE EDGE CRACKED FINITE PLATE SUBJECTED TO TENSILE STRESS

Lattif Shekher Jabur   Najah Rustum Mohsin

Iraq, Southern Technical University, Technical Institute-Nasiriya, Mechanical Technics Department.

E-mail: Lsh58@yahoo.com   Najahr2000@yahoo.com

ABSTRACT

A finite rectangular plate with double edge crack under uniaxial tension depends on the assumptions of Linear Elastic Fracture Mechanics LEFM and plane strain problem are studied in the present paper. The effect of crack position, crack oblique and the kinked crack orientation are investigated to predict if a crack starts to grow. These problems are solved by calculating the Stress Intensity Factor SIF for mode I (KI) and II (KII) near the crack tip theoretically using mathematical equations and numerically using finite element software ANSYS R15. A good agreement is observed between the theoretical and numerical solutions. The results show that the KI increases with increasing the relative crack length and tensile stress and these values are increased when the crack position draws near the plate edge while in case of parallel cracks the mutual shielding effect reduces KI in each crack. In mixed mode, it is shown that the maximum values of KI and KII occur at crack angle $\beta=0^o$ and 45°, respectively and the orientation of the kinked crack have significant effects on the KI and KII.

KeyWords: Double edge crack, SIF, crack oblique, ANSYS R15, kinked.

معامل شدة الأجهاد لصفيحة محددة ذات شق طرفي مزدوج معرضة لأجهاد شد

د. لطيف شخير جبر   نجاح رستم محسن

العراق ـ الجامعة التقنية الجنوبية ـ المعهد التقني في الناصرية ـ قسم التقنيات الميكانيكية

الملخص

في هذا البحث تم دراسة صفيحة محددة مستطيلة الشكل ذات شق طرفي مزدوج معرضة لأجهاد شد بأتجاه واحد أعتماداً على فرضيتي ميكانيكية الكسر المرن الخطية وأنفعال المستوي. تمت دراسة تأثير موقع الشق وزاوية الشق وزاوية الشق المتفرع للتنبوء بأمكانية نمو الشق. هذه المشاكل تم حلها بحساب معامل شدة الأجهاد للطور الأول و الثاني قرب قمة الشق نظرياً بأستخدام المعادلات الرياضية وعددياً بأستخدام برنامج العناصر المحددة ANSYS 15. لوحظ ان هنالك تطابق جيد بين الحل النظري والعددي. بينت النتائج ان الطور الأول لشدة الأجهاد يزداد بزيادة الطول النسبي للشق وأجهاد الشد وهذه القيمة تزداد عندما يقترب موقع الشق من حافة الصفيحة بينما في حالة الشقوق المتوازية فأن تأثير الدرع الواقي المشترك يقل من قيمة الطور الأول لكل شق. في الطور المختلط، لاحظنا ان القيمة القصوى للطور الأول والثاني تحدث عندما تكون زاوية الشق تساوي 0° و 45° على التوالي والميلان للشق المتفرع له تأثير واضح على قيمة الطور الأول والثاني لمعامل شدة الأجهاد.

1. INTRODUCTION

Recent development in engineering structures shows that small cracks in the body of structures can cause a failure despite of the authenticity of elasticity theory and strength of materials. As a result, fracture mechanics filed which is concerned with the propagation of cracks in materials has developed to study more about this subject, Ali et al. [1]. The crack may grow to cause structure failure due to low stress, which acts on a structure. Stress Intensity Factor (SIF) is a most important single parameter in fracture mechanics, which can be used to examine if a crack, would propagate in a cracked structure under particular loading condition, i.e. it controls the stability of the crack, Saleh [2].

No structure is entirely free of defects and even on a microscopic scale these defects act as stress raisers which initiate the growth of cracks. The theory of fracture mechanics therefore assumes the pre-existence of cracks and develops criteria for the catastrophic growth of these cracks. In a stressed body, a crack can propagate in a combination of the three opening modes that shown in Figure 1. Mode I represents opening in a purely tensile field while modes II and III are in-plane and anti-plane shear modes respectively. The most commonly found failures are due to cracks propagating predominantly in mode I, and for this reason materials are generally characterized by their resistance to fracture in that mode, Arencón and Velasco [3].

The double – edge cracked plate is a common specimen in research and practice for fracture mechanics. It has been studied by Bowie [4], who gave solutions for a circular hole with a single edge crack and a pair of symmetrical edge cracks in a plate under tension by using a conformal mapping technique, while Newman [5], using the boundary collocation method, and Murakami [6], used the body force method to analyze the tension problem for an elliptical hole with symmetrical edge cracks. Isida and Nakamura [7], made an analysis for a slant crack emanating from an elliptical hole under uniaxial tension and shear at infinity by using the force body method.

Yavuz et al. [8] analyzed multiple interacting cracks in an infinite plate to determine the overall stress field as well as SIF for crack tips and singular wedges at crack kinks. A perturbation approach for the elasticT-stress at the tip of a slightly curved or kinked crack based on used by Li et al. [9], while Saleh [2] analyzed and determined the KII of several crack configurations in plates under uniaxial compression using a two-dimensional Finite Element Method (FEM). Various cases including diagonal crack and central kinked crack are investigated with different crack's length, orientation and location. Antunes et al. [10] studied numerically the effect of crack propagation on crack tip fields. Spagnoli et al. [11] described the influence of the degree of crack deflection on the fatigue behavior and Ali et al. [1] utilized the SIF to determine the stress intensity near the tip of a crack using FEM. Recentllty, Mohsin

[12] studied the KI for center, single edge and double edge cracked finite plate subjected to tension stress to investigate the differences between the theoretical and numerical solutions.

Fracture mechanics is used to evaluate the strength of a structure or component in the presence of a crack or flaw, Fatemi [13]. In 1938 Westergaard solved the stress field for an infinitely sharp crack in an infinite plate (Figure 3). The elastic stresses were given by the equations, Rae [14]

$$\sigma_{xx} = \frac{KI}{\sqrt{2\pi r}} \cos\left(\frac{\theta}{2}\right) \left[1 - \sin\left(\frac{\theta}{2}\right) \sin\left(\frac{3\theta}{2}\right)\right] \quad \text{................(1)}$$

$$\sigma_{yy} = \frac{KI}{\sqrt{2\pi r}} \cos\left(\frac{\theta}{2}\right) \left[1 + \sin\left(\frac{\theta}{2}\right) \sin\left(\frac{3\theta}{2}\right)\right] \quad \text{.................(2)}$$

$$\tau_{xy} = \frac{KI}{\sqrt{2\pi r}} \cos\left(\frac{\theta}{2}\right) \sin\left(\frac{\theta}{2}\right) \cos\left(\frac{3\theta}{2}\right) \quad \text{.....................(3)}$$

i.e $\quad \sigma_{ij} = \left(\frac{KI}{\sqrt{2\pi r}}\right) f_{ij}(\theta), \quad \text{................(4)}$

where σ_{ij} is stress tensor, r is the distance from the crack tip, θ is the angle with respect to the plane of the crack, and f_{ij} are functions that are independent of the crack geometry and loading conditions.

From Saouma [15]

$$\sigma_{xx} = \sigma\sqrt{\frac{a}{2r}} \cos\frac{\theta}{2}\left(1 + \sin\frac{\theta}{2}\sin\frac{3\theta}{2}\right) + \cdots \quad \text{................(5)}$$

$$\sigma_{yy} = \sigma\sqrt{\frac{a}{2r}} \cos\frac{\theta}{2}\left(1 - \sin\frac{\theta}{2}\sin\frac{3\theta}{2}\right) + \cdots \quad \text{..............(6)}$$

$$\tau_{xy} = \sigma\sqrt{\frac{a}{2r}} \sin\frac{\theta}{2}\cos\frac{\theta}{2}\cos\frac{3\theta}{2} + \cdots \quad \text{.................(7)}$$

When $\theta = 0$, we have from (1) to (7)

$$\sigma_{ij} = \left(\frac{KI}{\sqrt{2\pi r}}\right) \quad \text{.............(8)}$$

$$\sigma_{xx} = \sigma_{yy} = \sigma\sqrt{\frac{a}{2r}} \quad \text{..........(9)}$$

$$\tau_{xy} = 0, \quad \text{............(10)}$$

then

$$\sigma_{xx} = \sigma_{yy} = \left(\frac{KI}{\sqrt{2\pi r}}\right) = \sigma\sqrt{\frac{a}{2r}} \quad \text{.............(11)}$$

Then, the KI of a finite plate under tension load is

$$KI = \sigma\sqrt{\frac{a}{2r}} \sqrt{2r\pi} = \sigma\sqrt{\pi a}, \quad \text{...........(12)}$$

Stress intensity solutions are given in a variety of forms, K can always be related to the through crack through the appropriate correction factor, Anderson [16]

$$K(I, II, III) = Y\sigma\sqrt{\pi a}, \quad \text{...................(13)}$$

where a: characteristic crack dimension and Y: dimensionless constant that depends on the geometry and the mode of loading.

When a body subjected to tension loading, the stress intensity factors for mode I and mode II to any planar crack oriented $90° − β$ (Figure 4) from the applied normal stress ($KI_β$ and $KII_β$) can be obtained depend on Sih et al. [17] as follow

$$KI_β = KI. \cos^2 β \quad \text{.......................(14)}$$

$$KII_β = KI. \cos β. \sin β , \quad \text{..............(15)}$$

where KI is the mode I stress intensity when $β = 0$.

Supposing that the crack in question forms an infinitesimal kink at an angle α from the plane of the crack, as Figure 5 illustrates. The local SIF at the tip of this kink differs from the nominal K values of the main crack. If we define a local x-y coordinate system at the tip of the kink , the local mode I and mode II stress intensity factors at the tip are obtained by summing the normal and shear stresses, respectively, at α, Anderson [16]:

$$KI_α = σ_{yy}\sqrt{2πr} = \left[\frac{3}{4}\cos\left(\frac{α}{2}\right) + \frac{1}{4}\cos\left(\frac{3α}{2}\right)\right] KI_β + \left[\frac{-3}{4}\left[\sin\left(\frac{α}{2}\right) + \sin\left(\frac{3α}{2}\right)\right]\right] KII_β \quad \text{.......(16)}$$

$$KII_α = τ_{xy}\sqrt{2πr} = \left[\frac{1}{4}\left[\sin\left(\frac{α}{2}\right) + \sin\left(\frac{3α}{2}\right)\right]\right] KI_β + \left[\frac{1}{4}\cos\left(\frac{α}{2}\right) + \frac{3}{4}\cos\left(\frac{3α}{2}\right)\right] KII_β , \quad \text{......(17)}$$

where $KI_α$ and $KII_α$ are the local SIF at the tip of the kink.

Figure 1: Fracture modes [3].

crack plate

dimensions.
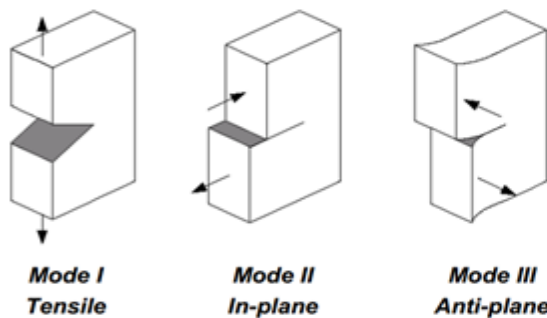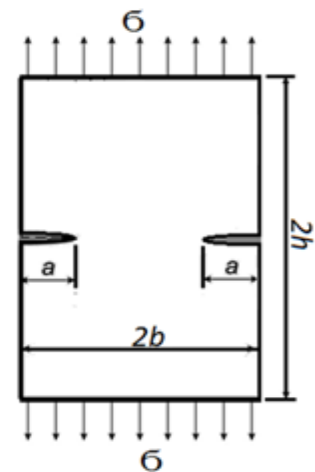
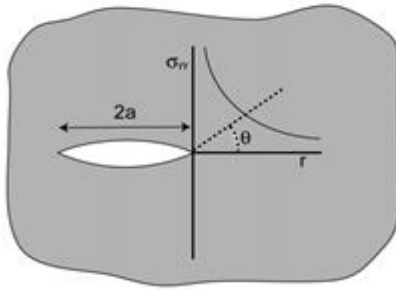Figure 2 Double edge

specimen   with

Figure 3: Crack with sharp edge [14] general case where the principal stress is
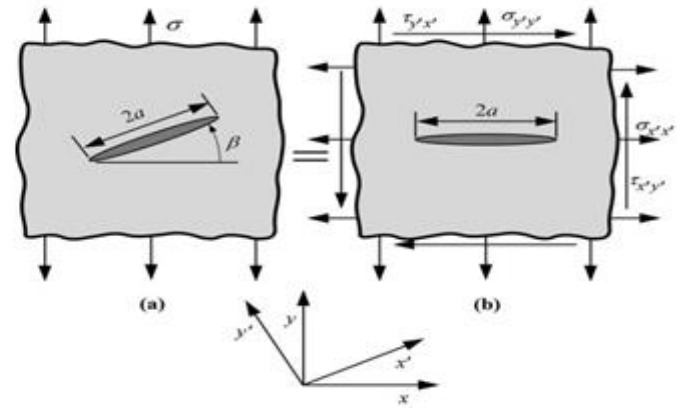
Figure 4: Through crack in an infinite plate for the not perpendicular to the crack plane[16].
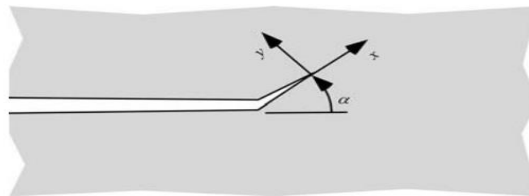

Figure 5: Infinitesimal kink at the tip of a macroscopic crack [16]

2. MATERIALS AND METHODS

Based on the assumptions of Linear Elastic Fracture Mechanics LEFM and plane strain problem, Double Edge Notch Tension (DENT) finite plate specimen as shown in Figure 2 is studied using theoretical and numerical solutions.

2.1. SPECIMENS MATERIAL

The material of plate specimens is a Carbon Steel with modulus of elasticity =202 E-3 MN/m^2, poison's ratio = 0.292 and density = 7820 Kg/m^3, Kulkarni [18].

2.2. SPECIMENS MODEL

To calculate the SIF in numerical and theoretical solutions, five models have been selected as follows

    I.   Double Edge Notch (DEN) is in the middle of the plate's length (Figure 6a and b).

    II.   DEN is in the various positions along Y-axis (Figure 6d).

    III.   Two parallel DEN are in the various positions along Y-axis (Figure 6e).

    IV.   DEN with crack orientation is in the middle of the plate's length (Figure 6f).

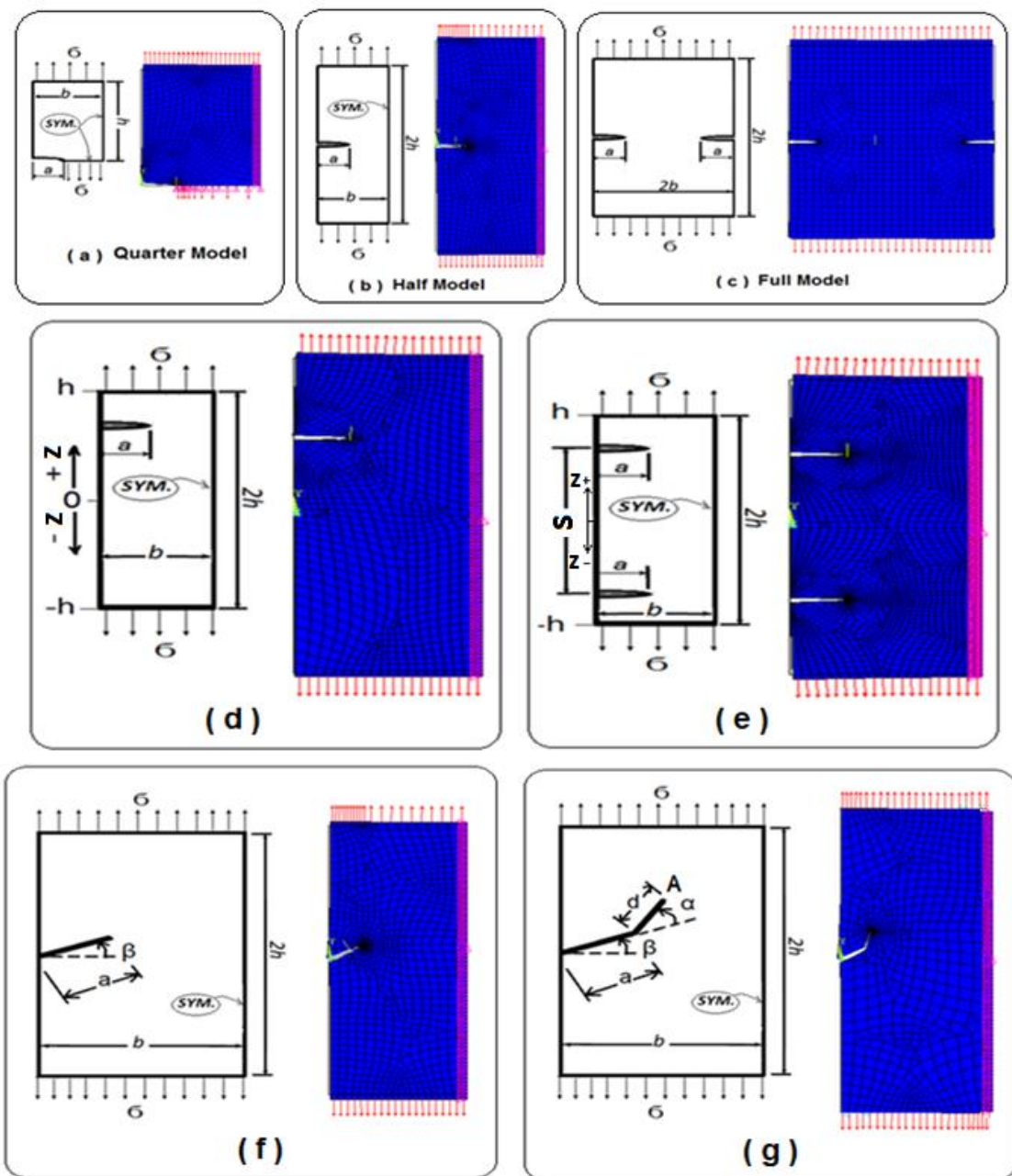   V.   DEN with crack orientation and kinked is in the middle of the plate's length (Figure 6g).

Figure 6: ANSYS models with mesh and dimensions.

2.3. THEORETICAL SOLUTION

For theoretical calculation, many researchers reported different equations for many cases to evaluate the SIF for double edge cracks. In this paper, the SIFs are theoretically calculated as follow : -

- KI values for model I, II and III (i.e. DENT without orientation ($\beta = 0$)) are calculated based on (13), where

  a) From Nassar [19]

$$Y = \left(\frac{\left(1.122 - 0.561\left(\frac{a}{b}\right) - 0.205\left(\frac{a}{b}\right)^2 + 0.471\left(\frac{a}{b}\right)^3 - 0.190\left(\frac{a}{b}\right)^4\right)}{\sqrt{1 - \left(\frac{a}{b}\right)}} \right) \quad \dots\dots\dots (18)$$

b) From Tada et al. [20]

$$Y = \left(1 + 0.122 cos^4\left(\frac{\pi a}{2b}\right)\right) \sqrt{\frac{2b}{\pi a} tan\left(\frac{\pi a}{2b}\right)} \quad \dots\dots\dots\dots\dots (19)$$

- Values of KI_β and KII_β for model IV (i.e. DENT with crack orientation) are calculated using equations (14)

  and (15), respectively.

- Values of KI_α and KII_α for model V (i.e. DENT with crack kinked) are calculated using equations (16) and

  (17), respectively.

2.4. NUMERICAL SOLUTION

Numerically, all the five models (as mensioned above) are solved to calculate the SIFs using finite element software ANSYS R15 with PLANE183 element as a discretization element.

2.5. PLANE183 ELEMENT DESCRPTION

PLANE183 is an ANSYS element with quadrilateral and triangle shape, plane strain behavior and pure displacement formulation. It is defined by 8 nodes (I, J, K, L, M, N, O, P) for quadrilateral element or 6 nodes (I, J, K, L, M, N) for triangle element, two degrees of freedom (Ux , Uy) at each node (translations in the X and Y directions) [21]. The geometry, coordinate system and node locations for this element are shown in Figure 7.
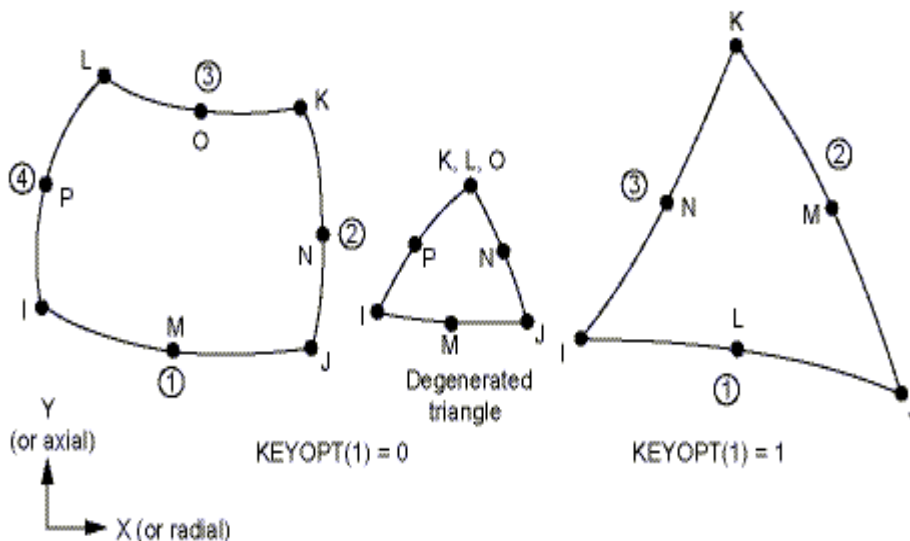

Figure 7: PLANE183 element geometry, coordinate system and node locations [21].

2.6. Applications

To explain the effect of the five cases that mention above on the SIFs, many cases are studied theoretically and numerically as reported in Table 1.

Table 1: The cases studied with the parameters, solution types and number of figures.

No. of Studied Cases	Changed Parameter in this case study		Other Parameters	Type of Solutions	Figure No.
	Name	Values			
I	a/b	0.1 to 0.6 with step 0.05	σ_t =200 Mpa b = 50mm h = 62.5mm	Theoretical and Numerical	8
	σ	50 to 250Mpa with step 50Mpa	b = 50mm h = 62.5mm a=15mm	Theoretical and Numerical	9
II	z	-50 to 50mm with step 5mm	σ_t =200 Mpa b = 50mm h=62.5mm a=15mm	Numerical	10
III	s	20mm to 100mm with step 10mm	σ_t =200 Mpa b = 50mm h=62.5mm a=15mm	Numerical	11
II and III	z	-50 to 50mm with step 5mm	σ_t =200 Mpa b = 50mm h=62.5mm a=15mm	Numerical	12
IV	β	-75° to 75° with step 5°	σ_t =200 Mpa b = 50mm h=62.5mm a=15mm	Theoretical and Numerical	13 and 14
V	(α+ β)	0°, 15°, 30° 45°, 60° 65°, 70° 75°, 80° 85°, 90°	σ_t =200 Mpa b = 50mm h=62.5mm a=10mm d=5mm β = 15°	Theoretical and Numerical	15 and 16
V	(α+ β)	0°, 15°, 30° 45°, 60° 65°, 70° 75°, 80° 85°, 90°	σ_t =200 Mpa b = 50mm h=62.5mm a=10mm d=5mm β = (15°, 45°, 75°)	Numerical	17 and 18

3. RESULTS AND DISCUSSIONS

3.1. Effect of relative crack length and tensile stress on the KI

Figures 8 and 9 explain the theoretical and numerical variation of KI for model I with different values of relative crack length (a/b) and tensile stresses (σ_t), respectively. It can be seen that increasing the ratio of a/b and σ_t leads to increasing the value of K_I in a high level. From these figures, it is clear that there is no significant difference between the Theoretical (Eq.18 and Eq.19) and numerical (Quarter and half model) results with a maximum discrepancy of 0.79%.
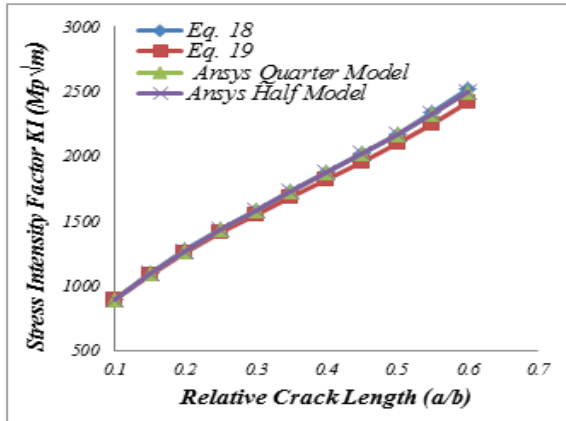
Figure 8: Theoretical and numerical Variation　　Figure 9: Theoretical and numerical Variation
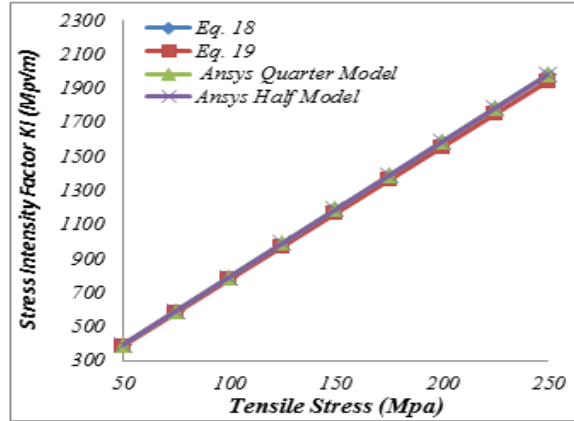
of KI with (a/b) ratio.　　　　　　　　of KI with σ_t.

3.2. Effect of DENT position on the KI

The variation of KI for model II with different edge crack positions along Y-axis (z) are shown in Figure 10. It can be seen that the KI values increases slightly from z = 0 to z = ±30mm, after that, KI values rises in a high level. Generally, maximum KI values appear at when the crack near the plate edge while the minimum values occur when its position at the middle of plate (i.e. z = 0).

Figure 10: Variation of KI with crack distance (z).

3.3. Effect of two parallel DENT position on the KI

Figure 11 illustrates the variation of KI for model III with various two parallel edge crack positions along Y-axis (s). From this figure, it can be seen that the KI values are increased with increasing the distance between the two parallel cracks (s).

In the other hand, Figure 12 explains a comparison between the effect of one and two edge crack positions along Y-axis on the KI from z = -50mm to z = +50mm. It is clear that the KI values for model II are greater than of model III at z = 0, after that, the difference decreases slightly from z=0 to z= ±40mm and vanished when z>±40mm. Generally, In case of parallel

cracks, the crack tends to shield one another and this mutual shielding effect reduces KI in each crack. The mutual shielding effect increase with decrease the distance between the two parallel cracks.
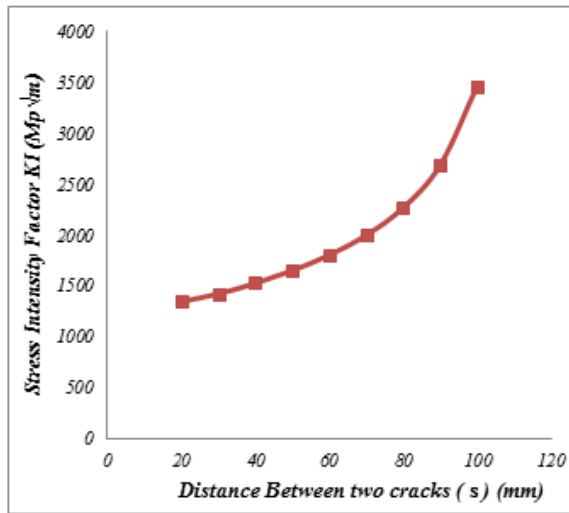

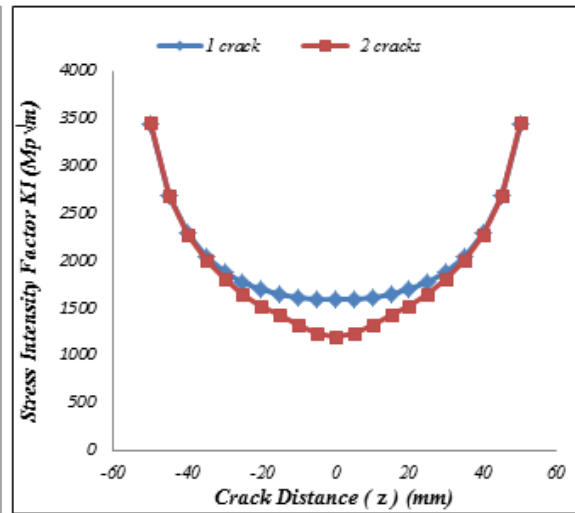| Figure 11: Variation of KI with the distance between two parallel cracks (s). | Figure 12: Variation of KI with crack distance for 1 and 2 cracks (z). |

3.4. Effect the DENT inclination angle on the KI and KII

The variation of KI and KII values with the double edge crack angle (β) for model IV are shown in figures 13 and 14, respectively. From these figures, it is too easy to see that the maximum KI and KII occur at $\beta = 0^\circ$ and $\beta = 45^\circ$, respectively. Furthermore, KI gradually decreases when $0^\circ > \beta > 0^\circ$ while KII gradually decreases when $45^\circ > \beta > 45^\circ$. In addition, it is shown that a small difference between KI values in numerical and theoretical solution but this difference will increase when calculate the KII especially when $60^\circ > \beta > 30^\circ$ and $-60^\circ < \beta < -30^\circ$. It is clear that the crack angle has a considerable effect on the KI and KII values as a result of the shear stresses and normal stresses depend on the angle values.
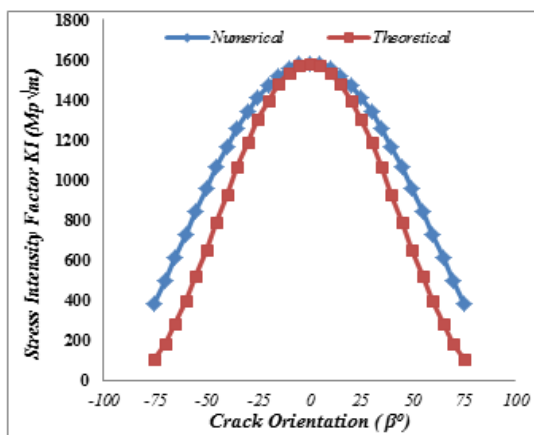

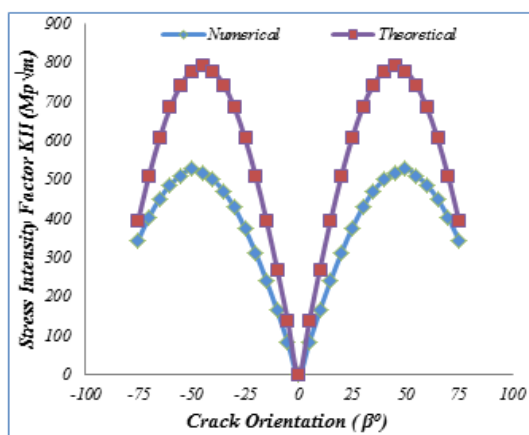| Figure 13: Variation of KI with the crack Orientation β°. | Figure 14: Variation of KII with the crack Orientation β°. |

3.5. Effect of the DENT inclination angle with kinked on the KI_A and KII_A

Figures 15 and 16 illustrate a compression between theoretical and numerical of KI_A and KII_A values (KI_A and KII_A= KI and KII at crack tip A, respectively as shown in Figure 6g) with variation of crack orientation plus kink angles (($\alpha+\beta$) = 0°, 15°, 30°, 45°, 60°, 75°, 80°, 85° and 90°)) at crack angle (β = 15°). From Figure 15 , it can be seen that there is a considerable effect between two curves when $\alpha < 0°$ after that, the difference decreases slightly and vanished at $\alpha > 60°$. In the other hand, From Figure 16, it is clear that there in no significant difference between theoretical and numerical values at $\alpha \leq 45°$ but the difference slightly increase after this angle.
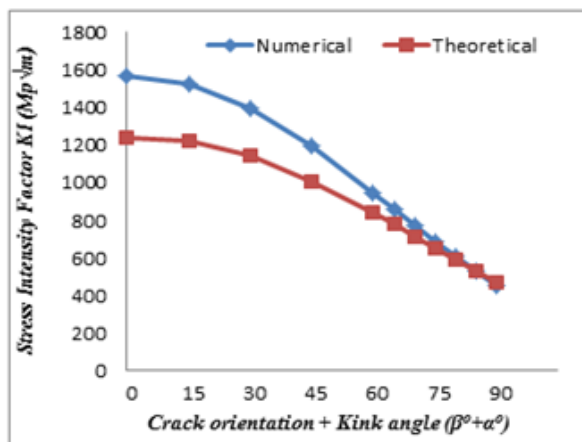

Figure 15: Theoretical and numerical variation
Figure 16: Theoretical and numerical variation
     of KI with the ($\beta°+\alpha°$) for ($\beta°$=15°).   of KII with the($\beta°+\alpha°$) for ($\beta°$=15°).

Furthermore, the variation of KI_A and KII_A with the (($\alpha+\beta$) = 0°, 15°, 30°, 45°, 60°, 75°, 80°, 85° and 90°) at crack angles (β = 15°, 45° and 75°) are explained in the Figures 17 and 18, respectively. Figure 17 illustrates that the increasing in the angles β and ($\beta+\alpha$) lead to slightly decrease in the KI_A values while, from figure 18, it can be seen that the increasing in the β lead to decrease in KII_A values. In addition, KII_A increases with the increase of ($\beta+\alpha$) angles until 60° and then it starts decreasing. Hence, maximum value of KI_A and KII_A occur at when ($\beta+\alpha$) = 0° and 60°, respectively. In fact, the mixed mode crack (crack with mode I and II) become a mode I crack only due to the crack tend to propagate perpendicular to the applied normal stress.
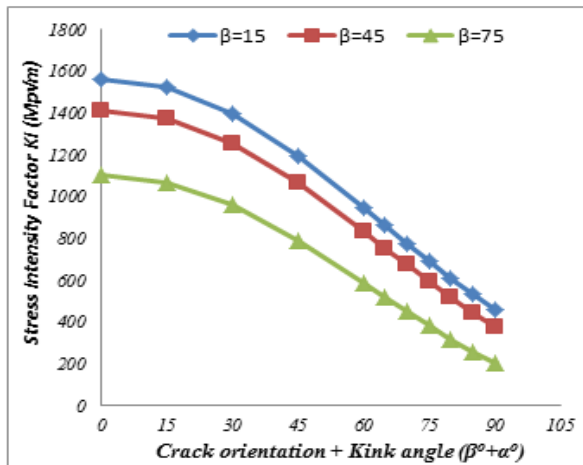
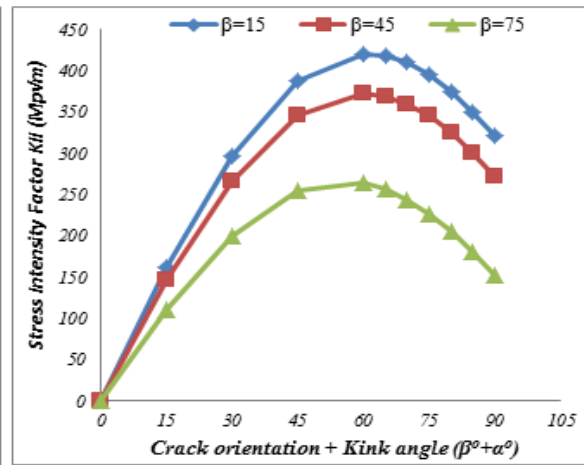Figure 17: Numerical variation of KI with the (β°+α°) for different β°.

Figure 18: Numerical variation of KII with the (β°+α°) for different β°.

Furthermore, Figures 19 and 20 are graphically illustrated Von-Mises stresses countor plots with the variation of the locations and angle of the crack. Figures 19a, b, c, d, and e explain the variation of Von-Mises stresses for DENT in the middle of the plate length, near the plate edge, parallel cracks, with angle and with kinked, respectively while the variation of Von-Mises stresses with different values of crack and kinked angles are illustrate in the Figures 20a, b, c, d and e. From these figures, it is clear that all cases mentioned above have a considerable effect on the plate stresses.
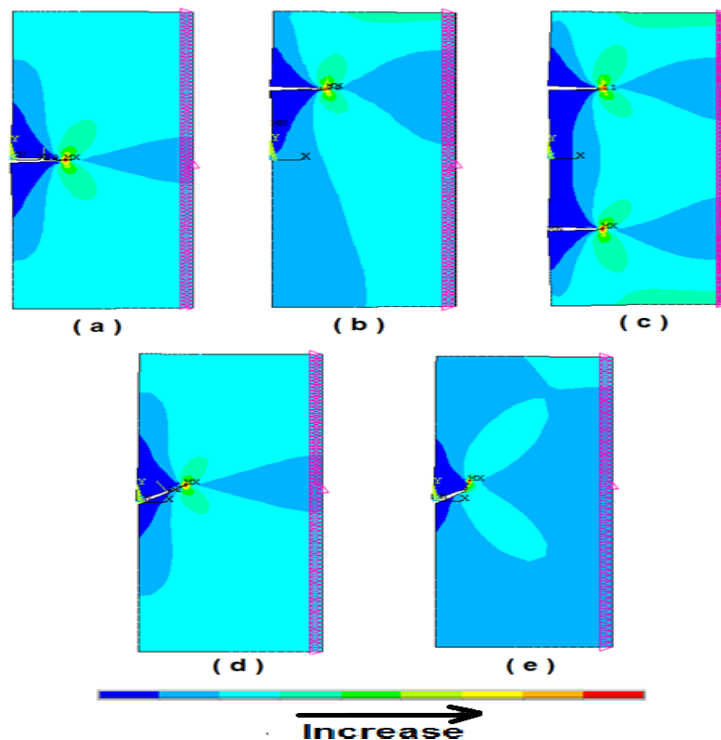

Figure 19: Countor plots of Von-Mises stress with the variation for double edge crack for different cases.
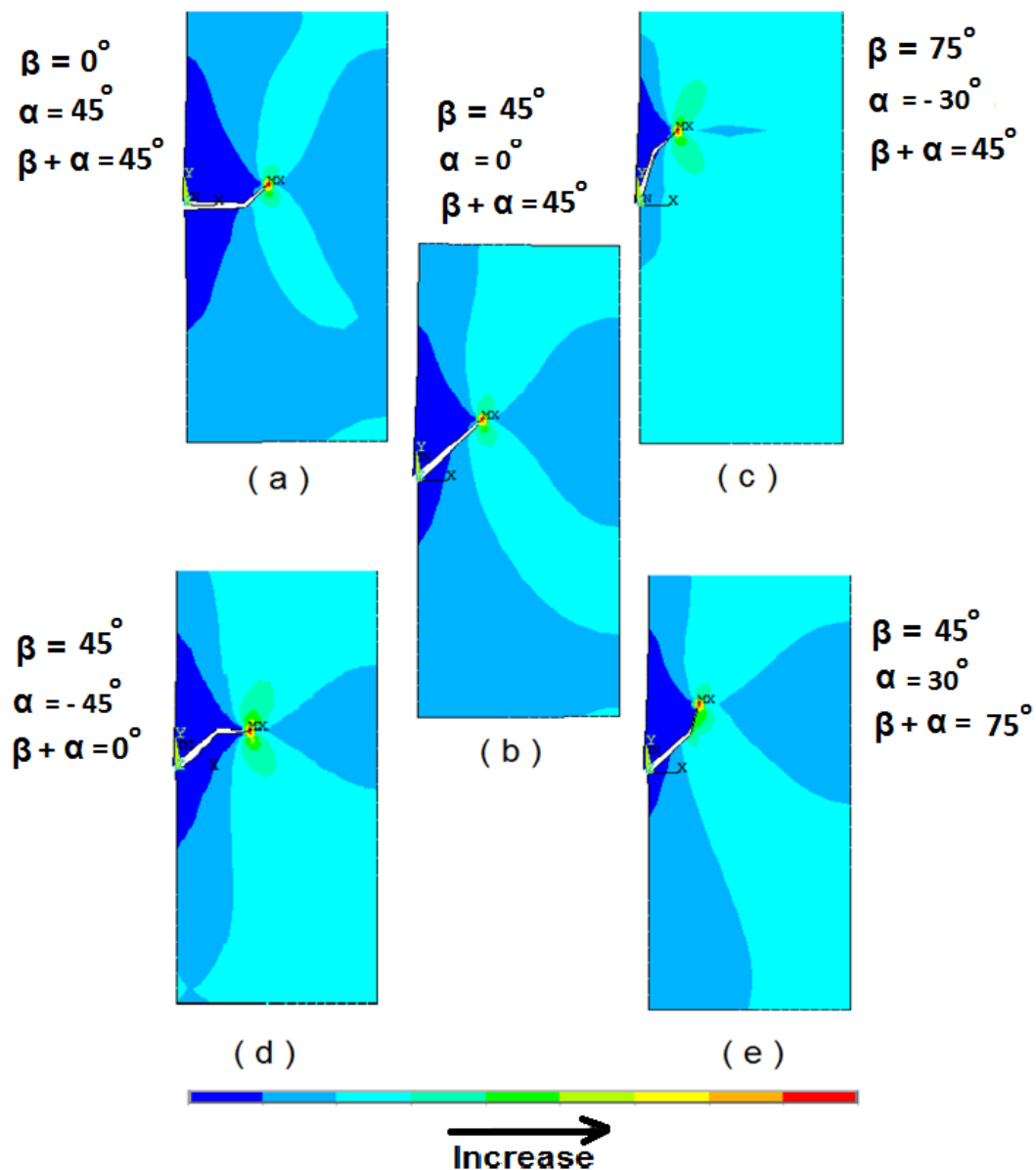
Figure 20: Countor plots of Von-Mises stress for different double edge crack orientations and kink angles.

4. CONCLUSIONS

The following conclusion can be drawn from the present study:

1- In all studied cases, a good agreement is observed between the theoretical and numerical results with a maximum discrepancy of 0.79%.

2- KI increases with increasing the relative crack length and tensile stress and when the crack position draw near the plate edge but this value decreased in the case of two parallel cracks as a result of the mutual shielding effect KI reduces in each crack.

3- The maximum values of KI and KII occur at crack angle $\beta=0^{\circ}$ and 45°, respectively. In addition, KII vanished at $\beta = 0^{\circ}$ and 90° while KI vanished at $\beta = 90^{\circ}$.

4- In kinked crack case, the maximum value of KIA and KIIA occur at $(\beta+\alpha) = 0o$ and $60o$, respectively. It was seen that the orientation of the kinked crack have a significant effects on the KI and KII.

5. REFERENCES

1. Z. Ali, K. E. S. Meysam, AsadiIman, B. Aydin, B. Yashar. Finite Element Method Analysis of Stress Intensity Factor in Different Edge Crack Positions, and Predicting their Correlation using Neural Network Method. Research Journal of Recent Sciences, Vol. 3(2), 69-73, 2014.

2. N. A. H. Saleh. A Study on Second Mode Stress Intensity Factor (KII) of Cracked Plates under Compression Load. Basrah Journal for Engineering Science, pp. 54-65, 2012.

3. D. Arencón and J. I. Velasco. Review, Fracture Toughness of Polypropylene-Based Particulate Composites. Journal of Materials, Vol. 2, pp. 2046-2094, 2009.

4. O. L. Bowie. Analysis of an Infinite Plate Containing Radial Cracks Originating at the Boundary of an Internal Circular Hole ", Journal of Math. & Phys. (MIT), Vol. 35, pp. 60-71, 1956.

5. J. C. Newman. An Improved Method of Collocation for the Stress Analysis of Cracked Plates with Various Shaped Boundary. NASA Technical Note TN D-6376, Langley Research Center, Hampton, VA, 1971. Aavailable at http://hdI.handle.net/2060/19710022830.

6. Y. Murakami. A Method of Stress Intensity Factor Calculation for the Crack Emanating from a Arbitrarity Shaped Hole or the Crack in the Vicinity of an Arbitrarity Shaped Hole. Trans. Jpn. Soc. Mech. Eng., Vol. 44:378, pp. 423-432, 1978.

7. M. Isida and Y. Nakamura. Edge Cracks Originating from an Elliptical Hole in a Wide Plate Subjected to Tension and in − Plan Shear. Trans. Jpn. Soc. Mech. Eng., VoL. 46:409, pp. 947-956, 1980.

8. A.K. Yavuz, S.L. Phoenix and S.C. TerMaath. An Accurate and Fast Analysis for Strongly Interacting Multiple Crack Configurations Including Kinked (V) and Branched (Y) Cracks. International Journal of Solids and Structures, Vol. 43, pp. 6727–6750, 2006.

9. D. F. Li, C. F. Li, H. Qing and J. Lu. The ElasticT-stress for Slightly Curved or Kinked Cracks. International Journal of Solids and Structures, Vol. 47, pp. 1753–1763, 2010.

10. F.V. Antunes, A.G. Chegini ,L.M. Correia and A.L. Ramalho. Effect of Crack Propagation on Crack Tip Fields. Frattura ed Integrità Strutturale, Vol. 25, pp. 54-60, 2013.

11. A. Spagnoli, A. Carpinteri and S. Vantadori. On a Kinked Crack Model to Describe the Influence of Material Microstructure on Fatigue Crack Growth. Frattura ed Integrità Strutturale, Vol. 25, pp. 94-101, 2013.

12. N. R. Mohsin. Comparison between Theoretical and Numerical Solutions for Center, Single Edge and Double Edge Cracked Finite Plate Subjected to Tension Stress. International Journal of Mechanical and Production Engineering Research and Development (IJMPERD), Vol. 5(2), pp. 11-20, 2015.

13. A. Fatemi. Fundamentals of LEFM and Applications to Fatigue Crack Growth –Chapter 6-LEFM & Crack Growth Approach. Available at https://www.efatigue.com/training/Chapter_6.pdf .

14. C. Rae. Natural Sciences Tripos Part II- Materials Science- C15: Fracture and Fatigue. Available at https://www.msm.cam.ac.uk/teaching/partII/courseC15/C15H.pdf .

15. V. E. Saouma. Lecture Notes in:Fracture Mechanics – Chapter 4, 2000. Available at http://civil.colorado.edu/~saouma/Lecture-Notes/lecfrac.pdf.

16. T.L.Anderson. Fracture Mechanics Fundamentals and Applications. Third Edition, Taylor &Francis Group, CRC Press, 2005.

17. G. C. Sih, P. C. Paris and G. R. Irwin. On Crakes in Rectilinearly Anisotrpic Bodies. International Journal of fracture Mechanics, Vol. 1, pp. 189-302, 1965.

18. S. G. Kulkarni. MachineDesign. McGraw-Hill Companies, Sixth Reprint, New Delhi, 2012.

18. A. A. Nassar. Evaluation of Critical Stress Intensity Factor (K_{IC}) for Plates Using New Crack Extension Technique. Eng. & Tech. Journal, Vol. 31, No. 4, 2013.

19. H. Tada, P. C. Paris and G. R. Irwin. The Stress Analysis of Cracks Handbook. Third Edition, ASME presses, 2000.

20. ANSYS. Release 15. Documentation.